FULL PAPER

Dalton
www.rsc.org/dalton

Complexation of alkali metal and alkaline earth ions by anthracene based fluorophores with one and two appended monoaza coronand receptors †

Jason P. Geue, Nicholas J. Head, A. David Ward and Stephen F. Lincoln *
Department of Chemistry, The University of Adelaide, Adelaide, SA 5005, Australia.
E-mail: stephen.lincoln@adelaide.edu.au

Received 21st October 2002, Accepted 23rd December 2002
First published as an Advance Article on the web 28th January 2003

The complexation of alkali metal ions by 13-[2-(10-ethyl-9-anthryl)ethyl]-1,4,7,10-tetraoxa-13-azacyclopentadecane, **1**, and 13-(2-{10-[2-(1,4,7,10-tetraoxa-13-azacyclopentadecanyl)ethyl]-9-anthryl}ethyl)-1,4,7,10-tetraoxa-13-azacyclopentadecane, **2**, to form fluorescent complexes in acetonitrile is reported. The fluorescence quantum yields, ϕ, are 0.25 and 0.03 for **1** and **2**, respectively. At 298.2 K and $I = 0.05$ mol dm^{-3} (NEt_4ClO_4) the $[M\mathbf{1}]^+$ complexes are characterised by complexation constants $K_1 = (1.28 \pm 0.01) \times 10^5$ ($\phi_1 = 0.71$), $(9.27 \pm 0.04) \times 10^4$ ($\phi_1 = 0.64$), $(1.73 \pm 0.02) \times 10^4$ ($\phi_1 = 0.60$), $(3.08 \pm 0.05) \times 10^3$ ($\phi_1 = 0.53$) and $(2.17 \pm 0.04) \times 10^3$ ($\phi_1 = 0.34$) dm^3 mol^{-1}, respectively, as M^+ changes from Li^+ to Cs^+. Fluorophore **2** forms weakly fluorescent $[M\mathbf{2}]^+$ and possibly the "sandwich" complex, $[M\mathbf{2}']^+$, which are jointly characterised by complexation constants $K_1 = (7.1 \pm 0.03) \times 10^5$, $(5.2 \pm 0.3) \times 10^5$, $(1.00 \pm 0.03) \times 10^4$ and $(1.8 \pm 0.2) \times 10^4$ dm^3 mol^{-1} for Li^+, Na^+, K^+ and Rb^+ and $[M_2\mathbf{2}]^{2+}$ characterised by $K_2 = (6.41 \pm 0.01) \times 10^4$ ($\phi_2 = 0.73$), $(4.84 \pm 0.01) \times 10^4$ ($\phi_2 = 0.53$), $(1.59 \pm 0.06) \times 10^3$ ($\phi_2 = 0.39$) and $(6.8 \pm 0.1) \times 10^2$ dm^3 mol^{-1} ($\phi_2 = 0.15$). (Cs^+ induced insufficient fluorescence in **2** for quantitative study.) The alkaline earths form more stable complexes with **1** and **2** characterised by K_1 and $K_2 \geq 10^7$ dm^3 mol^{-1}. The factors governing fluorescence and complex stability are discussed and the syntheses of **1** and **2** are described.

Introduction

Supramolecular systems whose fluorescence changes on complexing metal ions are the subject of increasing study because they potentially have use as logic systems and environmental and biomedical sensors.[1–5] Examples of such systems are the Ca^{2+} selective fluorophores, Quin-2 and Fura-2 and our Zn^{2+} selective fluorophores, Zinquin-A and Zinquin-E, which are widely used in intracellular studies.[6,7] One method for producing metal ion sensitive fluorophores adopts the "fluorophore–spacer–receptor" model in which the complexing of a metal ion by the receptor "switches off" quenching of the fluorophore to produce fluorescence through modulation of photoinduced electron transfer (PET).[1–3] In the process of designing new selective florophores we have studied the interaction of "anthracene–ethylene–azacoronand" systems **1** and **2** (Fig. 1) with alkali metal and alkaline earth metal ions (M^{m+}) in acetonitrile. The single receptor system **1** forms the $[M\mathbf{1}]^{m+}$ complex in which the fluorescence of anthracene is enhanced as the transfer of an electron from the azacoronand receptor nitrogen lone electron pair into the photoexcitation induced electronic vacancy in anthracene diminishes quenching. The two azacoronand receptors of **2** make possible three complexing modes as shown in Fig. 1. The formation of $[M\mathbf{2}]^{m+}$ leaves one receptor unoccupied and one nitrogen lone electron pair active to quench the fluorescence of anthracene. However, an isomer, $[M\mathbf{2}']^{m+}$, in which both receptors complex M^{m+} in a "sandwich" complex may also form and anthracene fluorescence quenching should be diminished. Such "sandwich" complexes have been reported for other coronand systems.[8] A third complex, $[M_2\mathbf{2}]^{2m+}$, may form in which two M^{m+} are complexed and anthracene fluorescence quenching should again be diminished. (The fluorescence of anthracene substituted at the 9 and 10 sites with a variety of receptor containing groups has previously been shown to be sensitive to the occupancy of the receptors.[9])

† Electronic supplementary information (ESI) available: figs. S1–S20: additional emission spectra. See http://www.rsc.org/suppdata/dt/b2/b210269b/

DOI: 10.1039/b210269b

Results and discussion

UV-visible and fluorescence spectra of 1 and 2 in acetonitrile

The UV-visible spectrum of **1** in acetonitrile at 298.2 K and $I = 0.05$ mol dm^{-3} (NEt_4ClO_4) shows a shoulder at 327 nm (1000 dm^3 mol^{-1} cm^{-1}) and absorbance maxima at 343 (2300), 360 (4900), 379 (8200) and 400 nm (7800 dm^3 mol^{-1} cm^{-1}). The corresponding data for **2** are a shoulder at 330 nm (1200 dm^3 mol^{-1} cm^{-1}) and absorbance maxima at 346 (2500), 362 (5100), 381 (8600) and 402 nm (8200 dm^3 mol^{-1} cm^{-1}). Small shifts to shorter wavelengths are observed in the spectra of **1** and **2** in the presence of 1.00×10^{-3} mol dm^{-3} alkali metal and alkaline earth metal ions, but these changes are insufficient for reliable estimation of the extent of complexation.

When excited at 375 nm in acetonitrile, **1** shows two fluorescence maxima at 406 nm (33) and 429 nm (30) and a shoulder at 452 nm (13) while **2** is characterised by maxima at 411 (3) and 435 nm (3) when excited at 383 nm (the relative fluorescence intensities are given in parentheses and refer to 3.00×10^{-6} mol dm^{-3} solutions at 298.2 K and $I = 0.05$ mol dm^{-3} (NEt_4ClO_4) and excitation and emission slitwidths of 10 and 5 nm, respectively). The relative fluorescence of **1** ($\phi = 0.25$) is substantially greater than that of **2** ($\phi = 0.03$) consistent with the fluorescence of the anthracene fluorophore arising from photoexcitation being quenched by electron transfer from the lone electron pair of an azacoronand receptor less efficiently in **1** than in **2**.

Alkali metal and alkaline earth ion complexation by 1 in acetonitrile

The formation of $[Li\mathbf{1}]^+$ significantly increases the relative fluorescence of **1** (Fig. 2); an effect which progressively diminishes in magnitude from $[Li\mathbf{1}]^+$ to $[Cs\mathbf{1}]^+$ (Figs. S1–S4 †). Nevertheless, the K_1 and ϕ_1 for $[Li\mathbf{1}]^+$ to $[Cs\mathbf{1}]^+$ are readily derived from these data as shown in Figs. 3 and 4 and Table 1. There is a systematic decrease in both K_1 and ϕ_1 for $[M\mathbf{1}]^+$ from $M^+ = Li^+$ to Cs^+ as the effective six-coordinate ionic radii of the alkali metal ions increases in the sequence: Li^+ (0.76 Å), Na^+ (1.02 Å), K^+ (1.38 Å), Rb^+ (1.52 Å) to Cs^+ (1.67 Å).[10] This is consistent with M^+ surface charge density dominating both the stability of

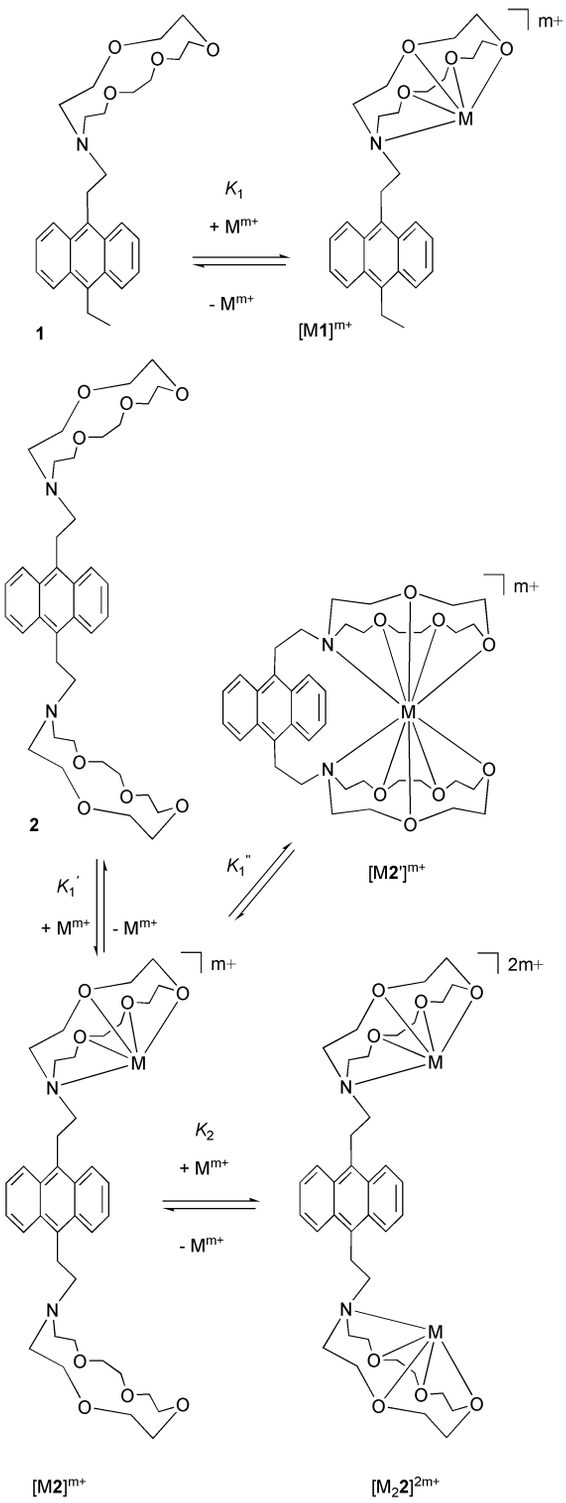

Fig. 1 The fluorophores **1** and **2** and possible M^{m+} complexation modes. For **2** $K_1 = K_1'(1 + K_1'')$.

the complexes and the strength of interaction of the metal ion with the lone pair of the azacoronand nitrogen and thereby the modulation of the PET quenching of the fluorescence of **1** in $[M\mathbf{1}]^+$. (A gas phase study shows that alkali metal ion surface charge density is the dominant factor determining coronate stability[11] in contrast to an earlier study which suggested that the coronand "hole size" match to the alkali metal ion size was a dominant factor determining coronate stability.[12] According to the latter reasoning the estimated 0.85–1.1 Å "hole radius" of 1,4,7,10,13-pentaoxacyclopentadecane should best accommodate Na^+ and form the most stable alkali metal coronate, which is the case in acetonitrile,[13] in contrast to Li^+ forming the most stable complexes with **1** and **2** in this study.)

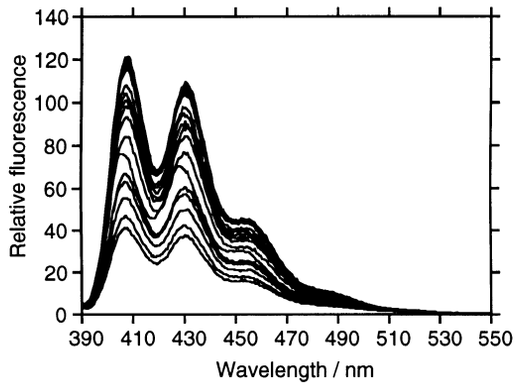

Fig. 2 The increase in emission of **1** (3.00×10^{-6} mol dm^{-3}) with $[Li^+]_{total}$ (1.00×10^{-6}–8.00×10^{-4} mol dm^{-3}) in acetonitrile (I = 0.05 mol dm^{-3}, NEt_4ClO_4) and 298.2 K, when excited at 381 nm. The lowest emission spectrum is that of **1**.

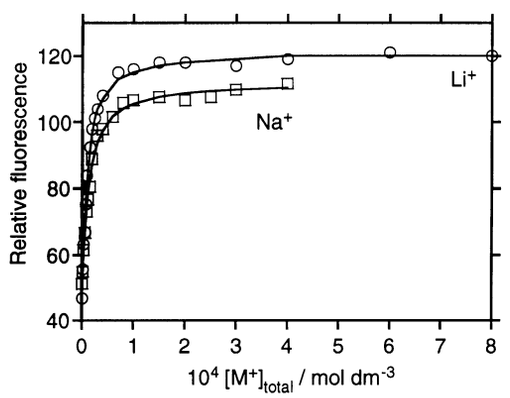

Fig. 3 Emission variation of **1** (3.00×10^{-6} mol dm^{-3}) at 407 nm with increase in $[Li^+]_{total}$ and $[Na^+]_{total}$ in acetonitrile (I = 0.05 mol dm^{-3}, NEt_4ClO_4) and 298.2 K when excited at 381 nm. The solid curves represent the best fit of the algorithm for the formation of $[M\mathbf{1}]^+$ to the experimental data points over the range 400–490 nm.

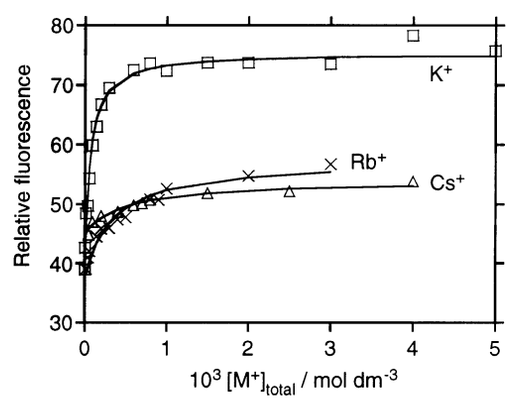

Fig. 4 Emission variation of **1** (3.00×10^{-6} mol dm^{-3}) at 407 nm with increase in $[K^+]_{total}$, $[Rb^+]_{total}$ and $[Cs^+]_{total}$ in acetonitrile (I = 0.05 mol dm^{-3}, NEt_4ClO_4) and 298.2 K when excited at 375, 386 and 382 nm, respectively. The solid curves represent the best fit of the algorithm for the formation of $[M\mathbf{1}]^+$ to the experimental data points over the range 400–490 nm.

The alkaline earths also induce substantial increases in fluorescence as shown for the formation of $[Mg\mathbf{1}]^{2+}$–$[Ba\mathbf{1}]^{2+}$ (Figs. S5–S8 †). The increase in fluorescence and formation of $[Mg\mathbf{1}]^{2+}$ follows the increase in $[Mg^{2+}]_{total}$ almost stoichiometrically consistent with $K_1 \geq 10^7$ dm^3 mol^{-1} (Fig. 5). Similar fluorescence variations occur for $[Ca\mathbf{1}]^{2+}$–$[Ba\mathbf{1}]^{2+}$ also consistent with $K_1 \geq 10^7$ dm^3 mol^{-1} (Figs. S9–S11 †). It is not possible to derive precise K_1 values for the alkaline earth complexes from the fluorimetric titration data because in the $[M^+]_{total}$ range where $[M\mathbf{1}^{2+}]$ varies the free $[M^{2+}]$ is very low so that small

Table 1 Complexation of alkali metal ions by **1** and **2** in acetonitrile at 298.2 K and $I = 0.05$ mol dm^{-3} (NEt_4ClO_4)

Fluorophore	Metal ion	K_1/dm^3 mol^{-1} [a]	ϕ_1 [b]	K_2/dm^3 mol^{-1}	ϕ_2 [b]
1	None		0.25		
	Li^+	$(1.28 \pm 0.01) \times 10^5$	0.71		
	Na^+	$(9.27 \pm 0.04) \times 10^4$	0.64		
	K^+	$(1.73 \pm 0.02) \times 10^4$	0.60		
	Rb^+	$(3.08 \pm 0.05) \times 10^3$	0.53		
	Cs^+	$(2.17 \pm 0.04) \times 10^3$	0.34		
2	None		0.03		
	Li^+	$(7.1 \pm 0.3) \times 10^5$	0.04	$(6.41 \pm 0.01) \times 10^4$	0.73
	Na^+	$(5.2 \pm 0.3) \times 10^5$	0.06	$(4.84 \pm 0.01) \times 10^4$	0.53
	K^+	$(1.00 \pm 0.03) \times 10^4$	0.02	$(1.59 \pm 0.06) \times 10^3$	0.39
	Rb^+	$(1.8 \pm 0.2) \times 10^4$	0.05	$(6.8 \pm 0.1) \times 10^2$	0.15
	Cs^+	[c]			

[a] For **2**, $K_1 = K_1'(1 + K_1'')$ as defined in Fig. 1. [b] Quantum yield. [c] Fluorescence change too small for accurate determination.

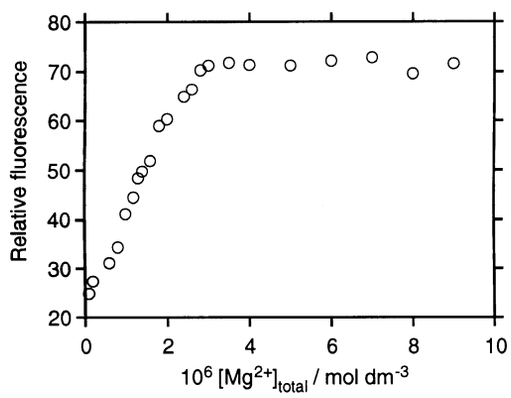

Fig. 5 Emission variation of **1** (3.00×10^{-6} mol dm^{-3}) at 406 nm with increase in $[Mg^{2+}]_{total}$ (1.00×10^{-7}–9.00×10^{-6} mol dm^{-3}) in acetonitrile ($I = 0.05$ mol dm^{-3}, NEt_4ClO_4) and 298.2 K when excited at 369 nm.

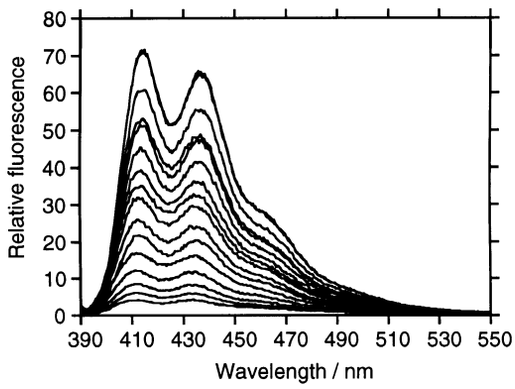

Fig. 6 The biphasic increase in emission of **2** (3.00×10^{-6} mol dm^{-3}) with $[K^+]_{total}$ (1.50×10^{-5}–3.00×10^{-3} mol dm^{-3}) in acetonitrile ($I = 0.05$ mol dm^{-3}, NEt_4ClO_4) and 298.2 K when excited at 380 nm. The lowest emission spectrum is that of **2**.

experimental errors produce large variations in $[M\mathbf{1}^{2+}]/[M^{2+}]$ and large errors in the data fits. Although the lack of quantitative fits of the algorithm for the formation of $[M\mathbf{1}]^{2+}$ to the fluorescence data precluded the quantitative derivation of K_1, $\phi_1 = 0.75$, 0.66, 0.67 and 0.66 were derived from the limiting fluorescence spectra obtained at high $[M^{2+}]_{total}$ for $M^{2+} = Mg^{2+}$, Ca^{2+}, Sr^{2+} and Ba^{2+}. The ϕ_1 for the complexes of the alkali metals are less than for those of the alkaline earths in the same period which may be a consequence of the higher surface charge densities of the alkaline earth metal ions more strongly engaging the azacoronand nitrogen lone pair and thereby decreasing the PET quenching of the anthracene fluorophore more effectively. However, the similarity of ϕ_1 for $[Li\mathbf{1}]^+$ and $[Mg\mathbf{1}]^{2+}$ may indicate that the maximum fluorescence has been reached for the fluorophore. {The alkaline earth effective six-coordinate ionic radii are: Mg^{2+} (0.72 Å), Ca^{2+} (1.00 Å), Sr^{2+} (1.18 Å) and Ba^{2+} (1.35 Å).[10]}

Alkali metal and alkaline earth ion complexation by 2 in acetonitrile

The biphasic variation of the fluorescence of **2** with increase in $[Li^+]_{total}$, $[Na^+]_{total}$, $[K^+]_{total}$ and $[Rb^+]_{total}$ (Figs. 6–8 and Figs S12–S14 †) indicates the formation of $[Li\mathbf{2}]^+$, $[Li\mathbf{2}']^+$ and $[Li_2\mathbf{2}]^{2+}$ for which the K_1, K_2, ϕ_1 and ϕ_2 characterising these complexes appear in Table 1 together with those for the analogous Na^+, K^+ and Rb^+ complexes. The K_1 for $[M\mathbf{2}]^+$ and $[M\mathbf{2}']^+$ decreases from $M^+ = Li^+$ to Rb^+ but not as systematically as for their **1** analogues possibly because of the formation of differing proportions of $[M\mathbf{2}']^+$. It is anticipated that $[M\mathbf{2}]^+$ should have a low fluorescence because of an uncomplexed receptor while $[M\mathbf{2}']^+$ might be expected to be more fluorescent as both receptors are complexed and quenching should be lessened. However, the observed ϕ_1 is low by comparison with ϕ_1 for $[M\mathbf{1}]^+$.

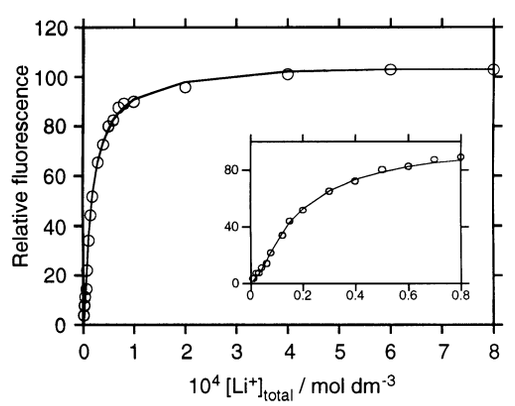

Fig. 7 The biphasic emission variation of **2** (3.00×10^{-6} mol dm^{-3}) at 411 nm with increase in $[Li^+]_{total}$ in acetonitrile ($I = 0.05$ mol dm^{-3}, NEt_4ClO_4) and 298.2 K when excited at 380 nm. The inset shows the emission variation over a small $[Li^+]_{total}$ range. The solid curves represent the best fit of the algorithm for the formation of $[Li\mathbf{2}]^+$, $[Li\mathbf{2}']^+$ and $[Li_2\mathbf{2}]^{2+}$ to the experimental data points over the range 400–490 nm.

This may indicate either that the proportion of $[M\mathbf{2}']^+$ is small or that $[M\mathbf{2}']^+$ is not significantly fluorescent because the hard acid alkali metal ions are dominantly complexed by the hard oxygens of each of the potentially pentadentate azacoronand receptor such that the lone electron pair of each nitrogen remains available to quench anthracene fluorescence. Either interpretation is consistent with the relatively large ϕ_2 values characterising $[M_2\mathbf{2}]^{2+}$ in which each M^+ is complexed by a single pentadentate azacoronand receptor and the nitrogen is probably more strongly complexed such that its lone pair is less available to quench anthracene fluorescence. There is a systematic decrease in both K_2 and ϕ_2 for $[M_2\mathbf{2}]^{2+}$ from $M^+ = Li^+$ to

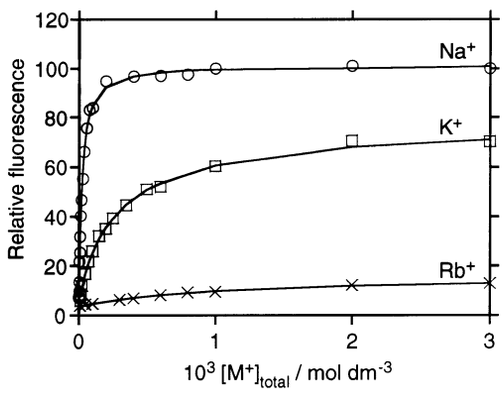

Fig. 8 The biphasic emission variation of **2** (3.00×10^{-6} mol dm^{-3}) at 411, 413 and 413 nm with increase in $[Na^+]_{total}$, $[K^+]_{total}$ and $[Rb^+]_{total}$ in acetonitrile ($I = 0.05$ mol dm^{-3}, NEt_4ClO_4) and 298.2 K when excited at 382, 380 and 376 nm, respectively. The solid curves represent the best fit of the algorithm for the formation of $[M\mathbf{2}]^+$, $[M\mathbf{2}']^+$ and $[M_2\mathbf{2}]^{2+}$ to the experimental data points over the range 400–490 nm. Due to the compressed scale the biphasic nature of the emission variation is not readily seen.

Rb^+ consistent with the coincident decrease in M^+ surface charge density dominating both the stability of $[M_2\mathbf{2}]^{2+}$ and the strength of interaction of the metal ion with the lone pair of the azacoronand nitrogen and thereby the modulation of the PET quenching of the fluorescence of **2** in $[M_2\mathbf{2}]^{2+}$.

The biphasic fluorescence increase of **2** accompanying the increase in $[Mg^{2+}]_{total}$ is almost complete when $[Mg^{2+}]_{total} = 2[\mathbf{2}]_{total} = 6.00 \times 10^{-6}$ mol dm^{-3} consistent with a close to stoichiometric complexation of Mg^{2+} (Figs. 9 and 10). This

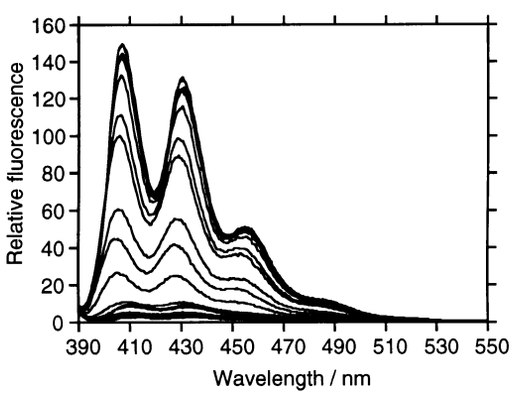

Fig. 9 The biphasic increase in emission of **2** (3.00×10^{-6} mol dm^{-3}) with $[Mg^{2+}]_{total}$ (5.00×10^{-7}–1.00×10^{-4} mol dm^{-3}) in acetonitrile ($I = 0.05$ mol dm^{-3}, NEt_4ClO_4) and 298.2 K when excited at 383 nm. The lowest emission spectrum is that of **2**.

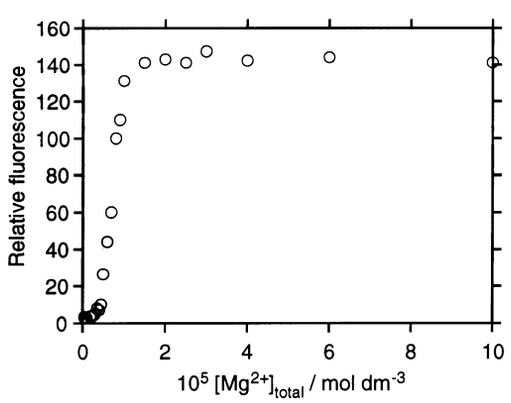

Fig. 10 The biphasic emission variation of **2** (3.00×10^{-6} mol dm^{-3}) at 406 nm with increase in $[Mg^{2+}]_{total}$ in acetonitrile ($I = 0.05$ mol dm^{-3}, NEt_4ClO_4) and 298.2 K when excited at 383 nm.

indicates the formation of $[Mg\mathbf{2}]^{2+}$ and $[Mg\mathbf{2}']^{2+}$ with a $K_1 \geq 10^7$ dm^3 mol^{-1} and a low ϕ_1 relative to ϕ_2 for $[Mg_2\mathbf{2}]^{4+}$ which also forms with $K_2 \geq 10^7$ dm^3 mol^{-1}, but this strong complexation prevents accurate quantification as discussed above for the alkaline earth complexes of **1**. Similar biphasic fluorescence increases of **2** accompany the increase in $[Ca^{2+}]_{total}$-$[Ba^{2+}]_{total}$ consistent with both K_1 and $K_2 \geq 10^7$ dm^3 mol^{-1} and $\phi_1 \ll \phi_2$ (Figs. S15–S20 †). While the lack of quantitative fits of the algorithm for the formation of $[M\mathbf{2}]^{2+}$ and $[M\mathbf{2}']^{2+}$ and $[M_2\mathbf{2}]^{4+}$ to the fluorescence data precludes the accurate derivation of the magnitudes of K_1, K_2 and ϕ_1 values, $\phi_2 = 0.81$, 0.77, 0.71 and 0.80 were derived when $M^{2+} = Mg^{2+}$, Ca^{2+}, Sr^{2+} and Ba^{2+} from the limiting fluorescence spectra obtained at high $[M^{2+}]_{total}$. The small variation of ϕ_2 may indicate that the maximum fluorescence has been reached for the fluorophore in these complexes. Their ϕ_2 are significantly larger than those for the analogous alkali metal complexes of **2** which is attributable to the higher surface charge densities of the alkaline earth metal ions more effectively modulating PET quenching.

Conclusion

For the alkali metals the K_1 and ϕ_1 for $[M\mathbf{1}]^+$ and K_2 and ϕ_2 for $[M_2\mathbf{2}]^{2+}$ decrease systematically consistent with the coincident decrease in M^+ surface charge density dominating the stabilities of $[M\mathbf{1}]^+$ and $[M_2\mathbf{2}]^{2+}$ and the extent of modulation of PET quenching of fluorescence of **1** and **2** in them. For the alkali metal $[M\mathbf{2}]^+$ and $[M\mathbf{2}']^+$ the decrease in K_1 with decrease in M^+ surface charge density is less systematic and the small ϕ_1 indicates that either little $[M\mathbf{2}']^+$ forms or that its PET modulation is weak. The higher K_1 and K_2 of the alkaline earth complexes of **1** and **2** are also in accord with these concepts as are ϕ_1 for $[M\mathbf{1}]^{2+}$ and ϕ_2 for $[M_2\mathbf{2}]^{4+}$ from which it appears that the higher alkaline earth surface charge densities, particularly for $[M_2\mathbf{2}]^{4+}$, increase the effectiveness of PET quenching possibly to the point where the maximum possible fluorescence is shown by the fluorophore. It is also noticeable that the spectra of $[M\mathbf{1}]^{2+}$ and $[M_2\mathbf{2}]^{4+}$ are significantly more structured and "anthracene like" than is the case for $[M\mathbf{1}]^+$ and $[M_2\mathbf{2}]^{2+}$ consistent with the higher surface charge density of the alkaline earths disengaging the electronic interactions between the anthracene substituents and the anthracene fluorophore to a greater extent than do the alkali metals. While **1** and **2** show insufficient selectivity between metal ions to be employed in selective sensor systems this study provides insight into the factors controlling fluorescent complex stability which it is planned to incorporate into more sophisticated sensor systems.

Experimental

General reagents

Perchorate salts (Fluka) were twice recrystallized from water and the anhydrous salt was obtained by drying to constant weight over P_2O_5 under vacuum prior to use. (**CAUTION**: Anhydrous perchlorate salts are potentially explosive and should be handled with care.) All solution preparations were carried out under an anhydrous nitrogen atmosphere. Acetonitrile used in UV-visible spectrophotometric and fluorimetric studies was purified by literature procedures[14] and dried and stored over 3Å molecular sieves.

Syntheses

9-Lithio-10-ethylanthracene, 9,10-di(2-iodoethyl)anthracene and methyltriphenoxyphosphonium iodide were prepared by methods similar to those in the literature.[15–17] Good ^{1}H, ^{13}C NMR and mass-spectrometric data were obtained. Solvents were purified by literature methods.[14] Other reagents were of good commercial quality and were used as received. All

manipulations and reactions were carried out under an anhydrous nitrogen atmosphere.

2-(10-Ethyl-9-anthryl)-1-ethanol

Ethylene oxide (0.7 cm^3, excess) was added dropwise with a cold syringe to freshly prepared 9-lithio-10-ethylanthracene (5.43 mmol) at 0 °C. The resultant yellow mixture was then allowed to warm to room temperature before it was poured onto ice (15 g). The precipitate that formed was filtered off, washed with diethyl ether (10 cm^3) and water (30 cm^3), then recrystallised from ethanol to afford the title compound as fluorescent yellow needles (562 mg, 41%). mp 148–150 °C. $\delta_H(CDCl_3)$: 1.44 (t, 3H, *J* 7.8 Hz, CH_2CH_3), 3.60 (q, 2H, *J* 7.8 Hz, CH_2CH_3), 3.95 (m, 2H, CH_2CH_2OH), 4.10 (m, 2H, CH_2CH_2OH), 7.53 (m, 4H, ArH), 8.36 (m, 4H, ArH). $\delta_C(CDCl_3)$: 15.48, 21.27, 31.12, 63.50, 125.00, 125.09, 125.13, 125.30, 128.54, 129.05, 130.30, 136.18. *m*/*z* (%); 250 ($M^{+\bullet}$, 27), 219 (86), 204 (24), 41 (100). Elemental analysis for $C_{18}H_{18}O$: C, 86.36; H, 7.25. Found: C, 86.02; H, 7.45%.

9-Ethyl-10-(2-iodoethyl)anthracene

Methyltriphenoxyphosphonium iodide (1.55 g, 3.4 mmol) was added to 2-(10-ethyl-9-anthryl)-1-ethanol (376 mg, 1.5 mmol) in dry *N*,*N*-dimethylformamide (5 cm^3) at 15 °C with stirring. After 1 h, methanol (5 cm^3), followed by water (5 cm^3), were added and the precipitate was filtered off, washed with methanol, then recrystallised from benzene to give the title compound as yellow needles (414 mg, 77%). mp 130–132 °C. $\delta_H(CDCl_3)$ 1.43 (t, 3H, *J* 7.5 Hz, CH_2CH_3), 3.43 (m, 2H, CH_2I), 3.61 (q, 2H, *J* 7.5 Hz, $ArCH_2CH_3$), 4.16 (m, 2H, $ArCH_2CH_2I$), 7.47–7.57 (m, 4H, ArH), 8.21 (m, 2H, ArH), 8.32 (m, 2H, ArH). $\delta_C(CDCl_3)$: 3.19, 15.40, 21.34, 33.50, 124.44, 125.12, 125.18, 125.72, 129.12, 129.23, 131.51, 136.79. *m*/*z* (%); 360 ($M^{+\bullet}$, 35), 233 (100), 204 (100), 189 (30). Elemental analysis for $C_{18}H_{17}I$: C, 60.02; H, 4.76. Found: C, 60.17; H, 4.95%.

13-[2-(10-Ethyl-9-anthryl)ethyl]-1,4,7,10-tetraoxa-13-azacyclopentadecane 1

1,4,7,10-Tetraoxa-13-azacyclopentadecane (150 mg, 0.62 mmol) was added to 9-ethyl-10-(2-iodoethyl)anthracene (100 mg, 0.28 mmol) in dry toluene (8 cm^3) and the solution was heated under reflux for 48 h. After cooling, the mixture was filtered and the solvent was removed *in vacuo*. The brown residue was redissolved in methanol (3 cm^3) and a 1.8 mol dm^{-3} solution of hydrogen chloride in methanol (1 cm^3) was added and the solvent was removed *in vacuo* to give a yellow powder (98 mg) which contained unreacted 1,4,7,10-tetraoxa-13-azacyclopentadecane hydrochloride as an impurity. An aqueous 10% sodium carbonate solution (2 cm^3) was added to the crude solid and it was extracted with dichloromethane (6 cm^3). The organic layer was washed with water (5 × 3 cm^3), the solvent was removed, and a 1.8 mol dm^{-3} solution of hydrogen chloride in methanol (1 cm^3) was added and the solvent was removed *in vacuo* to afford **1**·HCl as a pale yellow powder (67 mg, 49%). mp 166–168 °C. $\delta_H(CDCl_3)$: 1.41 (t, 3H, *J* 7.5 Hz, CH_2CH_3), 3.46–3.76 (m, 20H, 8 × CH_2O and 2 × $ArCH_2$), 4.00 (m, 2H, $ArCH_2CH_2N$), 4.32 (m, 4H, 2 × NCH_2CH_2O), 7.53 (m, 4H, ArH), 8.30 (d, 2H, ArH), 8.58 (d, 2H, ArH). $\delta_C(CDCl_3)$: 15.37, 21.17, 23.44, 52.09, 54.26, 65.79, 69.82, 70.60, 70.71, 124.89, 124.94, 125.05, 125.94, 126.49, 128.88, 129.86, 136.87. ESI-MS *m*/*z* (%); 453 (MH^+, 3), 233 (100), 205 (29), 100 (31), 43 (86). Elemental analysis for $C_{28}H_{38}NO_4Cl$: C, 68.91; H, 7.85; N, 2.87. Found: C, 68.61; H, 7.94; N, 2.83%.

13-(2-{10-[2-(1,4,7,10-Tetraoxa-13-azacyclopentadecanyl)ethyl]-9-anthryl}ethyl)-1,4,7,10-tetraoxa-13-azacyclopentadecane 2

1,4,7,10-Tetraoxa-13-azacyclopentadecane (404 mg, 1.84 mmol) was added to 9,10-di(2-iodoethyl)anthracene (208 mg, 0.43 mmol) in dry toluene (10 cm^3) and the solution was heated under reflux for 48 h. After cooling, the solvent was removed *in vacuo* and dichloromethane (15 cm^3) was added to the brown residue. The resulting solution was extracted with hydrochloric acid (4 × 10 cm^3, 0.10 mol dm^{-3}) which was then neutralised with potassium carbonate to give a pH = 11. This aqueous layer was extracted with chloroform (5 × 10 cm^3), the solvent was removed *in vacuo*, and a 1.8 mol dm^{-3} solution of hydrogen chloride in methanol (2 cm^3) was added. The solvent was again removed *in vacuo* to give a yellow powder that contained the desired compound and unreacted 1,4,7,10-tetraoxa-13-azacyclopentadecane as an impurity. Aqueous 10% sodium carbonate (4 cm^3) was added to the crude solid and the mixture was extracted with dichloromethane (3 × 6 cm^3). The combined extracts were washed with water (5 × 3 cm^3), the solvent was removed and a 1.8 mol dm^{-3} hydrogen chloride in methanol solution (2 cm^3) was added. The solvent was removed *in vacuo* to afford **2** as yellow–brown microcrystals (154 mg, 48%). mp 153 °C (decomp.). $\delta_H(CDCl_3)$: 3.49–3.77 (m, 36H, 16 × CH_2O and 2 × $ArCH_2$), 4.02 (m, 4H, 2 × $ArCH_2CH_2N$), 4.34 (m, 8H, 4 × NCH_2CH_2O), 7.60 (m, 4H, ArH), 8.61 (m, 4H, ArH). $\delta_C(CDCl_3)$: 23.68, 52.21, 54.31, 65.95, 69.96, 70.76, 70.87, 125.05, 126.35, 128.66, 129.92. ESI-MS *m*/*z* (%); 335 ($(MH_2)^{2+}$, 100), 669 ($MH^{+\bullet}$, 52), 691 ($(M + Na)^+$, 68). Elemental analysis for $C_{38}H_{61}N_2O_{10}Cl_2Na$: C, 57.07; H, 7.69; N, 3.50. Found: C, 56.74; H, 7.74; N, 3.35%.

UV-Visible spectroscopy

UV-Visible spectrophotometric absorbance data were collected at 0.5 nm intervals with a 2 nm slit bandwidth with a Cary 300 Bio double beam spectrophotometer. Solutions of **1** and **2** and reference containing the same supporting electrolyte were thermostatted at 298.2 ± 0.03 K in 1 cm pathlength stoppered silica cells sealed with tape to prevent entry of moisture. To determine the molar absorbances of **1** and **2**, the absorbances of four solutions of each in the concentration range (0.66–6.60) × 10^{-5} mol dm^{-3} were measured over the range 300–450 nm.

Fluorimetry

Fluorimetric measurements were carried out on solutions thermostatted at 298.2 ± 0.03 K in stoppered 1 cm pathlength silica cells sealed with tape to prevent entry of moisture using a LS50B fluorimeter with excitation and emission slit-widths of 10 nm and 5 nm, respectively. Complex stoichiometry and complexation constants were determined through non-linear least squares fitting of algorithms for the formation of 1 : 1, 1 : 1 and 2 : 1, 1 : 2, and 2 : 1 complexes to the relative fluorescence variation of **1** and **2** with alkali metal concentration at 0.5 nm intervals by using Method 5 of Pitha and Jones,[18] through the least squares regression routine DATAFIT[19] using the MATLAB formalism.[20] Using the Na^+–**2** system as an example, the observed fluorescence, *F*, is given by:

$$F = F_2[\mathbf{2}] + F_{Na2}[Na\mathbf{2}^+] + F_{Na2'}[Na\mathbf{2'}^+] + F_{Na22}[Na_2\mathbf{2}^{2+}]$$

where F_2, F_{Na2}, $F_{Na2'}$ and F_{Na22} are the relative fluorescences of the species whose concentrations are related through the complexation constants:

$$K_1 = ([Na\mathbf{2}^+] + [Na\mathbf{2'}^+])/([Na^+][\mathbf{2}]) \text{ and}$$
$$K_2 = [Na_2\mathbf{2}^{2+}]/\{([Na\mathbf{2}^+] + [Na\mathbf{2'}^+])[Na^+]\}$$

Quantum yields were determined from the derived fluorescence spectrum of each species using quinine in 0.50 mol dm^{-3} H_2SO_4 as the reference fluorophore and were corrected for solvent refractive index.[21]

Acknowledgements

We thank the Australian Research Council for supporting this research.

References

1 A. P. de Silva, H. Q. N. Gunaratne, T. Gunnlaugsson, A. J. M. Huxley, C. P. McCoy, J. T. Rademacher and T. E. Rice, *Chem. Rev.*, 1997, **97**, 1515; B. Valeur and I. Leray, *Coord. Chem. Rev.*, 2000, **205**, 3.
2 M. Kollmannsberger, K. Rurack, U. Resch-Genger and J. Daub, *J. Phys. Chem. A*, 1998, **102**, 10211; K. Rurack, J. L. Bricks, B. Schultz, M. Maus, G. Reck and U. Resch-Genger, *J. Phys. Chem. A*, 2000, **104**, 6171.
3 K. Yoshida, T. Mori, S. Watanabe, H. Kawai and T. Nagamura, *J. Chem. Soc., Perkin Trans. 2*, 1999, 393; H. Kawai, T. Nagamura, T. Mori and K. Yoshida, *J. Phys. Chem. A*, 1999, **103**, 660.
4 S. Fery-Forgues, M.T. le Bris, J.-P. Guetté and B. Valeur, *J. Phys. Chem. A*, 1988, **92**, 6233.
5 I. Leray, Z. Asfari, J. Vicens and B. Valeur, *J. Chem. Soc., Perkin Trans. 2*, 2002, 1429.
6 R. Y. Tsein, T. Possan and T. J. Rink, *J. Cell. Biol.*, 1982, **94**, 325; G. Grynkiewicz, M. Poenie and R. Y. Tsien, *J. Biol. Chem.*, 1985, **260**, 3440.
7 K. Hendrickson, T. Rodopoulos, P.-A. Pittet, I. Mahadevan, S. F. Lincoln, A. D. Ward, T Kurucsev, P. A. Duckworth, I. J. Forbes, P. D. Zalewski and W. H. Betts, *J. Chem. Soc., Dalton Trans.*, 1997, 3879; P. Coyle, P. D. Zalewski, J. C. Philcox, I. J. Forbes, A. D. Ward, S. F. Lincoln, I. Mahadevan and A. M. Roe, *Biochem. J.*, 1994, **303**, 781; P. D. Zalewski, I. J. Forbes, R. F. Seamark, R. Borlinghaus, W. H. Betts, S. F. Lincoln and A. D. Ward, *Chem. Biol.*, 1994, **1**, 153.
8 H. Sakamoto, K. Kimura, Y. Koseki, M. Matsuo and T. Shono, *J. Org. Chem.*, 1986, **51**, 4974; G. X. He, K. Kikukawa, T. Ikeda, F. Wada and T. Matsuda, *J. Chem. Soc., Perkin Trans. 2*, 1988, 719; J. Otsuki, T. Yamagata, K. Ohmuro, K. Araki, T. Takido and M. Seno, *Bull. Chem. Soc. Jpn.*, 2001, **74**, 333; T. D. James and S. Shinkai, *J. Chem. Soc., Chem. Commun.*, 1995, 1483.
9 A. P. de Silva, H. Q. N. Gunaratne and C. P. McCoy, *J. Am. Chem. Soc.*, 1997, **119**, 7891; H.-F. Ji, R. Dabestani and G. M. Brown, *J. Am. Chem. Soc.*, 2001, **122**, 9306; X. Xu, H. Xu and H.-F. Ji, *Chem. Commun.*, 2001, 2092; J. Kang, M. Choi, J. Y. Kwon and E. Y. Lee, *J. Org. Chem.*, 2002, **67**, 4384; T. Gunnlaugsson, A. P. Davis, J. E. O'Brian and M. Glynn, *Org. Lett.*, 2002, **4**, 2449; S. A. de Silva, B. Amorelli, D. C. Isidor, K. C. Loo, K. E. Crooker and Y. E. Peni, *Chem. Commun.*, 2002, 1360.
10 R. D. Shannon, *Acta Crystallogr., Sect. A*, 1976, **32**, 751.
11 M. B. More, D. Ray and P. B. Armentrout, *J. Am. Chem. Soc.*, 1999, **121**, 417.
12 H. K. Frensdorff, *J. Am. Chem. Soc.*, 1971, **93**, 600.
13 H. P. Hopkins and A. B. Norman, *J. Phys. Chem.*, 1980, **84**, 309.
14 D. D. Perrin and W. L. Armarego, *Purification of Laboratory Chemicals*, Permagon Press: Oxford, 3rd edn., 1988.
15 B. F. Duerr, Y.-S. Chung and A. W. Czarnik, *J. Org. Chem.*, 1988, **53**, 2120.
16 D. F. Evans and M. W. Upton, *J. Chem. Soc., Dalton Trans.*, 1985, 1141.
17 J. P. H. Veheyden and J. G. Moffatt, *J. Org. Chem.*, 1970, **35**, 2319.
18 J. Pitha and R. N. Jones, *Can. J. Chem.*, 1966, **44**, 3031.
19 T. Kurucsev, DATAFIT, University of Adelaide, 1980.
20 MATLAB 4.2b, The MathWorks, Inc., Cochituate Place, 24 Prime Park Way, Natick, Mass. 01760, USA.
21 W. H. Melhuish, *J. Phys. Chem.*, 1961, **65**, 229; C. H. Farnhi and T. V. O'Halloran, *J. Am. Chem. Soc.*, 1999, **121**, 11448.